PROCEEDINGS OF SCIENCE

Search for Neutral MSSM Higgs Bosons in the $\mu^+\mu^-$ final state with the CMS experiment in pp Collisions at $\sqrt{s} = 7$ TeV

Adrian Perieanu*
on behalf of the CMS Collaboration
I. Physikalisches Institut B, RWTH-Aachen
E-mail: Adrian.Perieanu@cern.ch

This paper presents a search for production of neutral Higgs bosons predicted by Supersymmetry using the $\mu^+\mu^-$ decay channel. The data from proton-proton collisions at $\sqrt{s} = 7$ TeV were recorded in 2011 with the CMS detector and correspond to an integrated luminosity of 4.96 fb^{-1}. The search is sensitive to SUSY Higgs boson production in association with a $b\bar{b}$ pair and via the gluon-gluon fusion process.

In the m_h^{max} scenario, this analysis excludes values of $\tan\beta$ between 16 and 26, at the 95% CL, for Higgs masses from 115 to 175 GeV/c^2. Less stringent limits in terms of $\tan\beta$ (between 26 and 40) are determined for higher values of the Higgs mass up to 300 GeV/c^2.

36th International Conference on High Energy Physics
4-11 July 2012
Melbourne, Australia

*Speaker.

PoS(ICHEP2012)089

1. Introduction

In the minimal supersymmetric extension of the standard model (MSSM), the Higgs sector contains the CP-odd neutral scalar A^0, two charged scalars $H^{\pm}$ and the two CP-even neutral scalars h^0 and H^0 [1, 2]. The neutral Higgs bosons will be collectively referred to as Φ^0 in this paper, unless specified otherwise. The phenomenology of the MSSM Higgs sector can be effectively described using only two parameters: m_{A^0}, the mass of the neutral scalar A^0, and $\tan\beta$, the ratio of the vacuum expectation values of the two doublets.

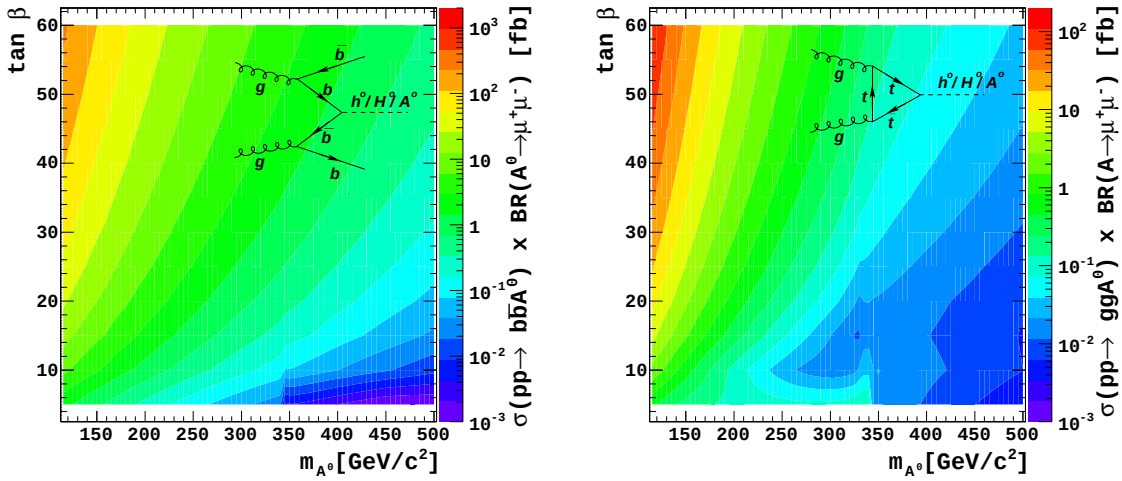

(a) (b)

Figure 1: *The A^0 production cross section times the $\Phi^0 \to \mu^+\mu^-$ branching ratio in the $(m_{A^0}, \tan\beta)$ plane for the $b\bar{b}A^0$ (a) and the ggA^0 (b) processes.*

In the MSSM, Neutral Higgs production $pp \to \Phi^0 + X$ at the LHC is dominated by $b\bar{b}$-associated production, where Φ^0 is produced together with a $b\bar{b}$ pair, $b\bar{b}\Phi^0$ (Fig. 1(a)), and the gluon-gluon (gg) fusion process, $gg\Phi^0$ (Fig. 1(b)). The associated production dominates over the gg fusion process at large values of $\tan\beta$ due to the enhance of coupling to b-quarks. Results of previous searches for the MSSM neutral Higgs bosons performed at LEP, Tevatron and LHC can be found in [3, 4, 5, 6]. Despite its lower branching ratio, the $\Phi^0 \to \mu^+\mu^-$ decay channel has a cleaner experimental signature due to the full reconstruction of the final state. The A^0 production cross sections multiplied by the branching ratio $A^0 \to \mu^+\mu^-$ in the $(m_{A^0}, \tan\beta)$ plane is presented in Fig. 1. The kinks observed for $m_{A^0} \sim 300$ GeV/c^2 are due to the opening of the $t\bar{t}$ decay channel.

The analysis is sensitive to both production mechanisms, $b\bar{b}$-associated and gluon-gluon fusion production and is performed using proton-proton collisions at $\sqrt{s} = 7$ TeV data corresponding to an integrated luminosity of 4.96 fb^{-1}. The results and the calculation of the exclusion limits rely on estimating the background from data. Monte Carlo (MC) simulation is used to estimate the signal selection efficiency and cross-check the data-driven background estimation methods.

2. The CMS Detector and Event Selection

A detailed description of the CMS detector can be found elsewhere [7]. The central feature of the CMS apparatus is a superconducting solenoid, providing a 3.8 T magnetic field. Within the field

volume are the silicon pixel and strip tracker, the crystal electromagnetic calorimeter (ECAL) and the brass/scintillator hadron calorimeter (HCAL). The tracks can be reconstruced with transverse momentum (p_T) as low as 100 MeV/c and a p_T resolution of 1% at 100 GeV/c. The energy resolution achieved by ECAL is $3\%/\sqrt{E_T/\text{GeV}}$ while in HCAL it is $100\%/\sqrt{E_T/\text{GeV}}$. Muons are measured in gas-ionization detectors embedded in the steel return yoke.

The process $\Phi^0 \to \mu^+\mu^-$ is characterized by the presence of two oppositely-charged muon tracks with high p_T. The events are assigned to one of the following three non-overlapping categories. *Category 1* contains events with at least one jet tagged as a b-jet candidate. In this category, b-tagging enhances the amount of signal events with respect to the Drell-Yan background. Such events are candidates for the process $\Phi^0 b\bar{b}$ shown in Fig. 1(a). In *Category 2* are selected the events where no b-jet candidate is reconstructed, but an additional third muon, μ_{3rd}, in the event is required as a signature of the b-quark semileptonic decay. Such events are also candidates for the process $\Phi^0 b\bar{b}$. The events that do not belong to *Category 1* or *Category 2* are forming the *Category 3*. This sample contains candidates of the gg-fusion process shown in Fig. 1(b).

The dataset is collected using a trigger that requires at least one muon candidate with a p_T above 24 GeV/c for the first part of the 2011 data sample and 30 GeV/c within $|\eta| < 2.1$ for the second part. Each event is required to contain at least one well reconstructed primary vertex (PV).

Muon candidates are reconstructed using both the tracker and the muon chamber information. The muons are required to be in the pseudorapidity range $|\eta| < 2.1$ and most energetic muon must have $p_T > 30$ GeV/c, whereas the second muon $p_T > 20$ GeV/c. A series of quality criteria presented in [8] need to be fulfill by the muon track in order to be accepted as good reconstructed candidates. The signal events have a rather small missing energy (E_T^{miss}) in the plane transverse to the beam direction. The analysis uses Particle Flow (PF) objects [9] to reconstruct jets and determine the E_T^{miss} in the event. The selection cut $E_T^{miss} < 30$ GeV is applied, as it provides a strong rejection of the $t\bar{t}$ background, but still preserves most of the signal events.

In the events where the Φ^0 boson is produced in association with a $b\bar{b}$ pair, the b-quarks fragment into jets that can be identified by an appropriate b-tagging algorithm [10]. Jets are reconstructed using the *anti*-k_T jet selection algorithm [11] with a radius of 0.5 in the $|\eta_{jet}| < 2.4$ region with $p_{T\,jet} > 20$ GeV/c. In addition they should be well separated from the muon track by a distance of $\Delta R_{\mu-jet} > 0.5$ in pseudorapidity and azimuthal angle. To perform the b-tag, tracks associated to a jet are ranked according to their impact parameter significance, d. The second largest d in the jet is taken as the discriminator variable for the whole jet. Events that fail the b-tag selection are classified in *Category 2* if an additional muon candidate, μ_{3rd}, is found in the event. In signal events produced in association with $b\bar{b}$, the μ_{3rd} is expected to be produced in b-hadron semileptonic decays. It is required to have a $p_T > 3$ GeV/c in $|\eta| < 2.4$ range, be well separated with respect to each of the two hard muons, $\Delta R > 0.5$, and fulfill additional track quality cuts [8].

In Fig. 2 the di-muon invariant mass distribution is shown for each of the three categories, both for data and simulated backgrounds. The expected di-muon distribution for the decay $\Phi^0 \to \mu^+\mu^-$, with $m_{A^0} = 150$ GeV/c^2 and $\tan\beta = 30$ is superimposed for illustration. Signal events were simulated using Pythia [12] over a large range of values of m_{A^0} and $\tan\beta$.

After the selection mentioned before, most of the remaining background events are due to the Drell-Yan process. The $b\bar{b}Z^0$ process is the irreducible background for $b\bar{b}\Phi^0$ associated production. Another important source of background is $t\bar{t}$ production (for *Category 1*) and $W^\pm W^\pm$ production

(for *Category 3*), with t-quark or W bosons decays leading to muons in the final state. Other less important sources of background that were still considered in the analysis, are the $Z^0(\tau^+\tau^-, e^+e^-)$ or $W^{\pm}$ plus jets production processes, $W^{\pm}Z^0$, Z^0Z^0, QCD and single t production [8].

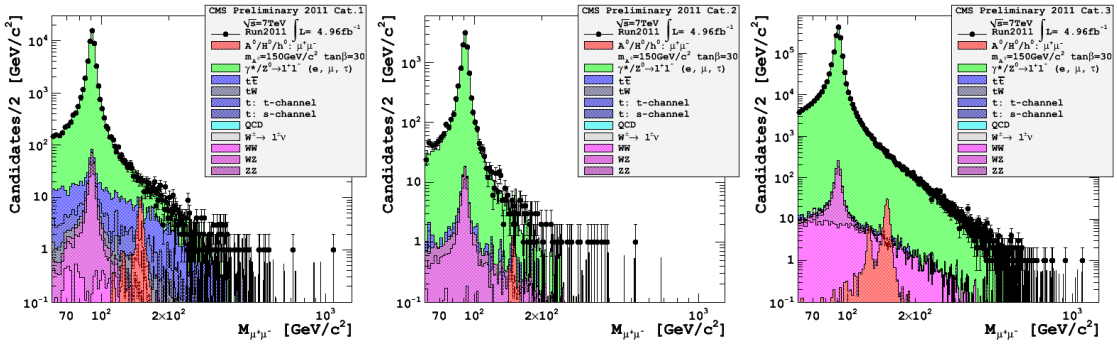

(a) (b) (c)

Figure 2: *The $\mu^+\mu^-$ invariant mass distribution for Category 1 (a), 2 (b) and 3 (c). The expected signal for the decay $\Phi^0 \to \mu^+\mu^-$, with $m_{A^0} = 150$ GeV/c^2 and $\tan\beta = 30$ is superimposed.*

3. Background Estimation and Exclusion Limits

The search for a Higgs signal and the exclusion limit calculation are performed using a data driven approach with the background contribution determined from a fit to the data. The shape of the expected signal (A^0, h^0 or H^0), for the various values assumed for m_{A^0} and $\tan\beta$ is determined by a fit to the invariant mass distribution of the simulated signal events. The distribution is modeled by the function F_{sig}, which is a linear combination of three Breit-Wigner (BW) functions normalized to unity, taking into account the experimental resolution. The relative contribution of the three functions, F_{BWh^0}, F_{BWH^0} and F_{BWA^0} is parametrised as $F_{sig} = a \cdot F_{BWh^0} + b \cdot F_{BWH^0} + (1-a-b) \cdot F_{BWA^0}$. The parameters that represent the mass and width of the three BW functions, and the relative contribution of the three Higgs bosons are determined from the fit on simulated signal events.

For each signal choice, a linear combination of the functions describing the expected Higgs boson contribution and the background is fit to the data. In this procedure the parameters that describe the shape of the signal, determined in the previous step, are kept constant and only the relative amount of signal to background is varied. As the Drell-Yan is the dominant background process, the background fit function model is given by a BW function plus the photon exchange term proportional to $1/M^2_{\mu^+\mu^-}$. Defining $x = M_{\mu^+\mu^-}$, the function describing the background is $F_{bkg} = e^{\lambda x}\left(\frac{f_{BWZ^0}}{N_{norm1}} \cdot \frac{\Gamma_{Z^0}}{(x-M_{Z^0})^2+\frac{\Gamma^2_{Z^0}}{4}} + \frac{(1-f_{BWZ^0})}{N_{norm2}} \cdot \frac{1\text{GeV/c}^2}{x^2}\right)$ where $e^{\lambda(x)}$ describes the exponential part of the parton density function and $N_{norm\,i}$ is given by the integral of corresponding function in the chosen mass range. The parameters Γ_{Z^0} and M_{Z^0} are previously determined from a fit of the di-muon invariant mass around the Z^0 peak for each category of events. They are used as fixed parameters in F_{bkg}. The detector resolution is included in the fitted width. The function used to fit the data is $F = N \cdot \left[(1 - f_{Background}) \cdot F_{sig} + f_{Background} \cdot F_{bkg}\right]$. The term $f_{Background}$ and the quantities f_{BWZ^0} and λ contained in F_{bkg} are left to vary, whereas all previously determined parameters related to F_{sig} are kept constant. The parameter N, the normalization factor, multiplied with $f_{Background}$ returns the number of expected background events. An example of the fit for data events from

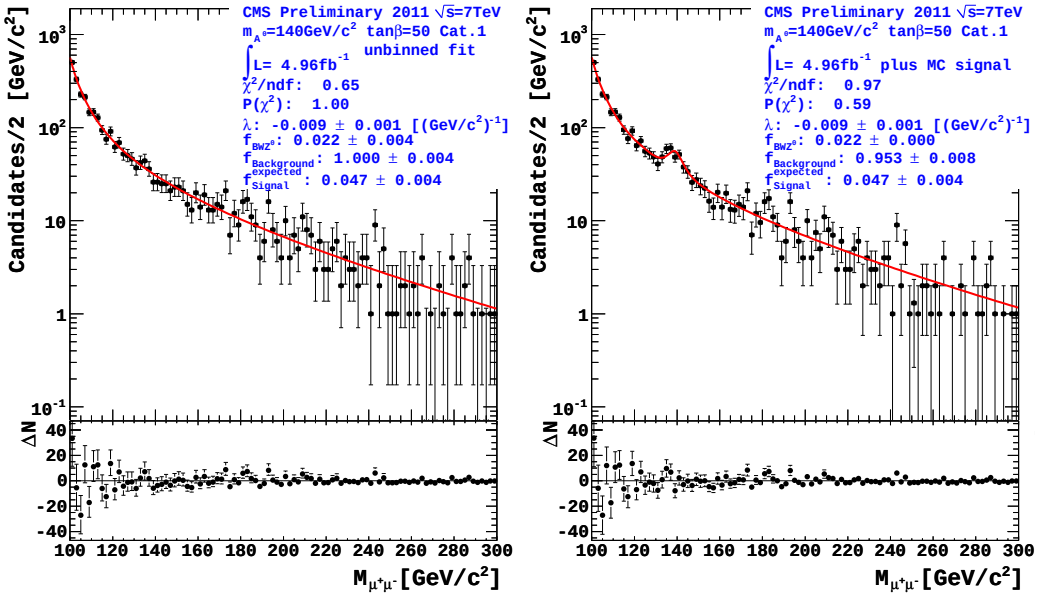

(a) (b)

Figure 3: *Fit of the di-muon spectrum of data from Cat. 1 (a). A test of the fit procedure is illustrated in (b) where the expected Monte Carlo signal is artificially added to the data.*

Category 1 with the signal hypothesis $m_{A^0} = 140$ GeV/c^2 and $\tan\beta = 50$ is shown in Fig. 3(a). A test of the fit stability is illustrated in Fig. 3(b) where the expected signal for $m_{A^0} = 140$ GeV/c^2 and $\tan\beta = 50$ is artificially added to the data. In this case the quantity $f_{Background}$ determined from the fit, multiplied by the number of events in the histogram, reproduces the expected number of background events determined from the histogram of Fig. 3(a) within one standard deviation. The term $f_{Signal}^{expected}$ is calculated as the ratio between the number of selected MC signal events and the number of events in data with $100 < M_{\mu^+\mu^+} < 300$ GeV/c^2. This ensures that the background calculation is robust against the possible presence of signal events in the data.

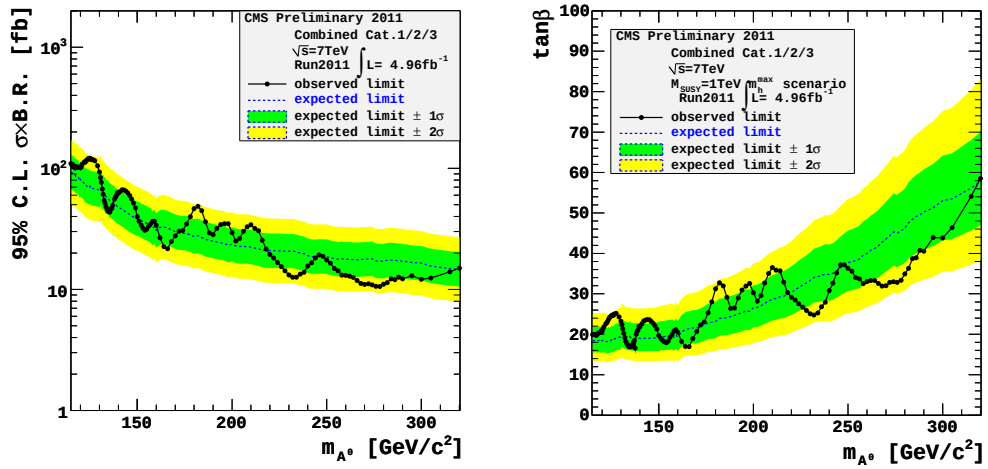

(a) (b)

Figure 4: *The combined exclusion limit for the MSSM production cross-section times the B.R. at 95% CL (a) and its projection in the (m_{A^0}, $\tan\beta$) plane (b). The excluded regions are above the curves.*

The systematic uncertainty of the fit method is found to vary between 1% and 6% for different m_{A^0} values. Additional dominant uncertainties [8] are due to measurement of the E_T^{miss} (1.8%), the

b-tagging (3.6%), the integrated luminosity (2.2%), the parton distribution function (up to 3%), the renormalization and factorization scale (from 5% to 13%) as well as the theoretical cross-section (from 16% to 20%) which is needed when limits in terms of $\tan\beta$ and m_{A^0} are calculated.

No evidence for the neutral MSSM Higgs bosons was found therefore exclusion limits are calculated. The confidence level (CL) of the exclusion limit in the (m_{A^0}, $\tan\beta$) plane is calculated, using the Asymptotic CL algorithm [13] for events of *Category 1, 2* and *3*. The value of $\tan\beta$ at which the CL exceeds 95% is chosen for each mass point to perform the final limit calculation. The limit on the rate is then transformed into a limit on the cross section times the branching ratio to muons. Using this limit on the cross section and the knowledge of the cross section in the MSSM, the limit can be projected on $\tan\beta$ to exclude a certain region in the ($m_A^0, \tan\beta$) parameter plane. In Fig. 4 the combined exclusion limits are presented. The results for each category alone can be seen in [8]. No deviation from the $+2\sigma$ uncertainty band is observed.

4. Conclusions

The search for the neutral MSSM Higgs bosons A^0, h^0 and H^0 decaying to $\mu^+\mu^-$ is performed assuming the m_h^{max} scenario. The proton-proton collisions data analyzed here were recorded at $\sqrt{s} = 7$ TeV with the CMS detector and correspond to 4.96 fb^{-1}. No evidence of the MSSM m_h^{max} scenario Higgs boson production is found within the sensitivity of the analysis.

The exclusion limits are obtained by fitting the background contribution from data while the Monte Carlo simulation is used only to compute the expected signal contribution. The analysis excludes at 95% CL in the m_h^{max} scenario values of $\tan\beta$ between 16 and 26 for Higgs mass from 115 to 175 GeV/c^2. Less stringent limits in terms of $\tan\beta$ (between 26 and 40) are determined for higher values of the Higgs mass up to 300 GeV/c^2.

References

[1] I. Aitchinson, *Supersymmetry and the MSSM: An Elementary Introduction*, [hep-ph/0505105].
[2] S. Martin, *A Supersymmetry Primer*, [hep-ph/9709356].
[3] L. Suter, *Combined CDF and D0 upper limits on MSSM Higgs boson production in proton-antiproton collisions at the Tevatron*, [arXiv:1110.1920].
[4] ALEPH, DELPHI, L3 and OPAL Collaborations, LEP Working Group for Higgs Boson Searches, *Search for neutral MSSM Higgs bosons at LEP*, *Eur. Phys. J.* **C47** 547-587 [hep-ex/0602042].
[5] CMS Collaboration, *Search for Neutral MSSM Higgs Bosons Decaying to Tau Pairs in pp Collisions at $\sqrt{s} = 7$ TeV*, *Phys. Rev. Lett.* **106** (2011) 231801.
[6] ATLAS Collaboration, *Search for neutral MSSM Higgs bosons decaying to tau pairs in proton-proton collisions at $\sqrt{s} = 7$ TeV with the ATLAS detector*, *Phys. Lett.* **B705** 174-192 [arXiv:1107.5003].
[7] CMS Collaboration, *The CMS experiment at the CERN LHC*, *JINST* **3** S08004.
[8] CMS Collaboration, *Search for Neutral MSSM Higgs Bosons in the $\mu^+\mu^-$ final state with the CMS experiment in pp Collisions at $\sqrt{s} = 7$ TeV*, CMS-PAS-HIG-12-011.
[9] CMS Collaboration, *Particle-Flow Event Reconstruction in CMS and Performance for Jets, Taus and MET*, CMS-PAS-PFT-09-001.
[10] CMS Collaboration, *b-Jet Identification in the CMS Experiment*, CMS-PAS-BTV-11-004.
[11] M. Cacciari, G. P. Salam and G. Soyez, *The Anti-k(t) jet clustering algorithm*, *JHEP* **0804** 063 [arXiv:0802.1189].
[12] T. Sjöstrand, S. Mrenna and P. Z. Skands, *PYTHIA 6.4 Physics and Manual*, *JHEP* **0605** 026 [hep-ph/0603175].
[13] G. Cowan et al., *Asymptotic formulae for likelihood-based tests of new physics*, *Eur. Phys. J.* **C71** 1554.